Chapter 2
Intensification of Adsorption Process in Porous Media

Lingai Luo

Abstract This chapter presents research and ideas on the design and shape optimization of porous media and related process devices for rapid and efficient gas adsorption. In particular, we will focus on the intensified temperature swing adsorption (TSA) process by employing several methods such as thermal conductivity promoter, thermoelectric elements and cyclic operating mode, which illustrate well different aspects of the notion of intensification. Other methods for intensification of adsorption processes will be briefly discussed also in the context of pressure swing adsorption (PSA), of electro-thermal swing adsorption (ESA), and of the use of circulating fluidized bed (CFB). Finally, the design of a porous material or system with multi-scale internal geometry for gas adsorption and storage will be presented, expressing necessary compromises between mass and heat transport characteristics.

> The strong and the weak (lines) have their fixed and proper places (in the diagrams); their changes, however varied, are according to the requirements of the time (when they take place)….When a series of changes has run all its course, another change ensues. When it obtains free course, it will continue long.
> —the Book of Changes, translated by James Legge

L. Luo (✉)
Laboratoire de Thermocinétique de Nantes, UMR CNRS 6607, Centre National de la Recherche Scientifique (CNRS), Polytech'Nantes, La Chantrerie, Rue Christian Pauc, BP 50609, 44306 Nantes Cedex 03, France
e-mail: lingai.luo@univ-nantes.fr

L. Luo (ed.), *Heat and Mass Transfer Intensification and Shape Optimization*,
DOI: 10.1007/978-1-4471-4742-8_2,

2.1 Introduction

In this chapter, I will present my research work carried out during the years on the adsorption processes in porous media, and my reflexions and efforts on their intensification. As we know, the adsorption processes involve a porous solid and a fluid mixture (a gas or a liquid, but only gas phase application will be considered in the following), mainly for the purpose of separation. This can be best understood with the example illustrated in Fig. 2.1, the entire cycle of the separation process is composed of two half-cycles: the cold half-cycle for adsorption and the hot half-cycle for desorption. In the cold half-cycle, the gas mixture to be separated passes through the adsorbent bed where the target species will be adsorbed, providing in the outflow a depleted concentration of that species. Once the adsorption capacity (saturation) is reached, the hot half-cycle begins for the regeneration of the adsorbent by reflux or purge gas. The adsorption and desorption proceed one after another in cycles, leading to the separation of the gas mixture.

The cyclic or periodic characteristic of the separation processes is fundamental, from the viewpoint of intensification, because it determines the duration of the cycles, hence the productivity. As a result, the main objective of our work is to *shorten the duration of the cycles* so as to intensify the process. The "*temporal intensification*" aspect is highlighted here, whereas the aspects of geometrical or spatial intensification are also involved.

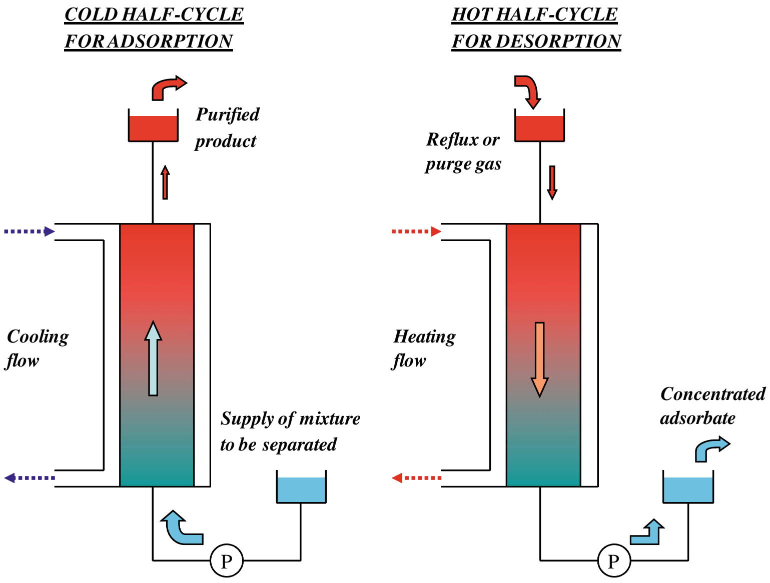

Fig. 2.1 Adsorption/desorption cycle in an adsorbent bed by varying the temperature

One important feature of adsorption processes is that mass and heat transfer characteristics are strongly related. Low temperature promotes the adsorption while high temperature encourages the desorption (regeneration of the adsorbent). Hence the productivity of such a process depends strongly on the frequency at which we are capable of varying the temperature of the adsorbent bed, i.e. heating or cooling the adsorbent as quickly as possible to reach the temperature set-points for adsorption and desorption, respectively.

Meanwhile, the adsorption/desorption time depends also on the inner structure of the porous media, i.e. the transport time for the gas molecules passing through the meso and the micro pores and finally reaching the nano-pores where the adsorption actually happens. The porosity of the porous media should also be carefully determined because more solid means better heat conduction but less pore volume for adsorption capacity. As a result, how to design a structured porous material that offers an optimal distribution of pore volume among different scales for the easiest and uniform access of gas molecules towards nano-pores is also a very important issue for improving the productivity of the adsorption processes.

In this chapter, I will present various efforts that I made for the intensification of gas adsorption processes in porous media. Special emphasis will be given to the rapid temperature swing adsorption (TSA) process using various intensification methods. Other adsorption processes such as pressure swing adsorption (PSA), and electro-thermal swing adsorption (ESA) will also be briefly discussed within the framework of parametric separation (Le Goff and Tondeur 1978; Grévillot 1986; Tondeur and Grévillot 1986). Finally, I will present an effort on the design and shape optimization of a porous material for gas adsorption and storage.

2.2 Rapid Thermal Swing Adsorption

Temperature swing adsorption (TSA) is commonly used for gas purification, for example the treatment of volatile organic compounds (VOCs) from gaseous streams. In conventional TSA processes, the heating and desorption are usually effected by flowing steam or hot gas through the bed and for cooling cold gas is used instead. Steam desorption is usually fast and efficient by itself, but requires lengthy subsequent drying and cooling stages. In all cases, this implies that flowing of large quantities of gas through the bed is required, and it takes a long time, usually several hours.

How to heat and cool the adsorbent bed more rapidly so as to significantly increase the productivity of a TSA process?

I am going to discuss successively in this section various methods of intensification that I have used, including:

- enhancing the overall heat transfer in the particle bed by using “thermal conductivity promoters”, i.e. sheets of compacted natural graphite;

- using *thermoelectric elements* (Peltier effect) to accelerate the dynamics of temperature changes;
- using a pertinent operating mode for the adsorption–desorption cycle;
- augmenting the separation by Cycling-Zone Adsorption.

2.2.1 Thermal Conductivity Promoters

As I have discussed in the introduction, the key factor that limits the duration of a TSA cycle is the inefficient heat transfer, which is directly linked to the poor thermal conductivity of the adsorbent. For example, the thermal conductivity of activated carbon is generally around 0.2 $W \cdot m^{-1} \cdot K^{-1}$, which could be considered as non-thermal conductive material. Meanwhile, the thermal conductivity of graphite (e.g. compacted natural exfoliated graphite) is much higher, up to 350 $W \cdot m^{-1} \cdot K^{-1}$ (Bonnissel et al. 2001a). *Can it be used as thermal conductivity promoters to improve the heat conduction in porous media?*

In fact, this idea is not new. At the beginning of this research, I had intensive discussions with some of our partners, especially the team of B. Spinner (PROMES at Perpignan, France) and the team of F. Meunier (LIMSI at Orsay, France), who have worked on this issue in the context of refrigeration machinery by adsorption or by gas–solid reaction.

One of the methods proposed by these teams is to fabricate the mixture of solid particles (Coste et al. 1983) by intimate mixing and compression of natural exfoliated graphite powder with the active product, e.g. activated carbon (SNEA-LCL 1991), zeolite, metallic salt (Spinner et al. 1993), etc. The major shortcoming of this approach is that to obtain a significant enhancement of thermal conductivity, there should be a large proportion of graphite, 40 % of the final volume for example. However, with this proportion, the compression of this mixture results in a cohesive solid block having very low permeability, which is not acceptable for gas adsorption.

Another method is to use highly conductive fins made of metal (foam or metal straws), evenly distributed in the porous media (Douss and Meunier 1988; Guilleminot and Meunier 1989). This method is more interesting, since these materials can ensure a good continuity of conduction and take a small volume fraction or mass fraction of promoter (about 10 %) at the same time. The disadvantages are the chemical sensitivity of the metal, the difficulty of packing, the loss of compactness and the risk of non-uniform packing with the consequence of a wide residence time distribution.

By compacting unidirectionally the natural exfoliated graphite particles, I have realised compacted graphite sheets with different densities and strong anisotropic conductivity properties. The experimental measurements and comparison with data of some typical metals (Table 2.1) indicate that the perpendicular[1]

---

[1] “perpendicular” and “parallel” are relative to the direction in which the compression has taken place.

Table 2.1 Thermal conductivities of natural exfoliated graphite and corresponding metals conductivity (Bonnissel et al. 2001a)

Bulk density ($kg \cdot m^{-3}$)	Porosity	Parallel conductivity ($W \cdot m^{-1} \cdot K^{-1}$)	Perpendicular conductivity ($W \cdot m^{-1} \cdot K^{-1}$)	Metal ($W \cdot m^{-1} \cdot K^{-1}$)
200	0.91	8	25	Stainless steel (13.4)
400	0.82	9	60	Carbon steel (60)
800	0.64	8	170	Magnesium (156)
1,200	0.45	7.5	280	Aluminum (237)
1,400	0.36	7	340	Copper (401)

conductivity increases with the bulk density to an impressive value of 340 $W \cdot m^{-1} \cdot K^{-1}$ at 1,400 $kg.m^{-3}$, close to that of copper (401 $W \cdot m^{-1} \cdot K^{-1}$). The parallel thermal conductivity however, is two orders of magnitude lower compared to the perpendicular thermal conductivity, but still much higher than that of activated carbon particles.

Another feature of compacted exfoliated graphite sheets is their small density and thermal capacity combined with a great thermal conductivity. The expression of the thermal diffusivity α combines three parameters ($\alpha = \lambda / \rho C_p$). As shown in Table 2.2, high values of perpendicular diffusivity could be obtained (2.86×10^{-4} $m^2 \cdot s^{-1}$ at 1,400 $kg \cdot m^{-3}$), higher than that of metals like copper (1.17×10^{-4} $m^2 \cdot s^{-1}$) or even silver (1.74×10^{-4} $m^2 \cdot s^{-1}$). In the parallel direction, the thermal diffusivity is similar to that of common metals (carbon steel; lead; zinc, etc.).

This property of high thermal diffusivity is essential for all transient operations where low inertia is desirable, and makes them better than metallic sheets for the present purpose.

Encouraged by this observation, I designed with my colleagues an adsorption column consisting of thin activated carbon particle layers separated by thin compacted graphite sheets, named active composite with intensified thermal

Table 2.2 Thermal diffusivity of the compacted natural exfoliated graphite and corresponding metals diffusivity (Bonnissel et al. 2001a)

Bulk density ($kg \cdot m^{-3}$)	Porosity	Parallel diffusivity (10^6 $m^2 \cdot s^{-1}$)	Perpendicular diffusivity (10^6 $m^2 \cdot s^{-1}$)	Metal (10^6 $m^2 \cdot s^{-1}$)
200	0.91	47	147	Aluminum (97)
400	0.82	26	176	Copper (117)
800	0.64	12	250	Gold (127)
1,200	0.45	7.4	274	Silver (174)
1,400	0.36	5.9	286	Silicon carbide (230)

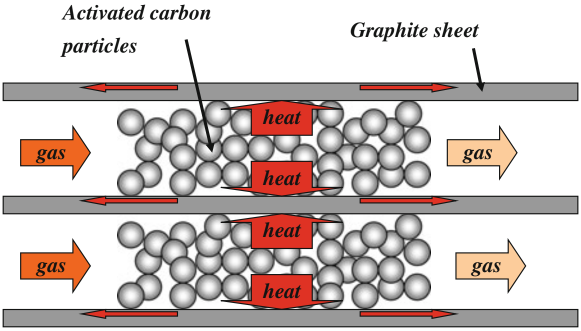

Fig. 2.2 Laminated structure of active composite with intensified thermal properties

properties (Fig. 2.2). The optimization of the characteristic dimensions of such module is based on the *equipartition of the values of characteristic transfer time* $\tau = L^2/\alpha$ along the graphite sheet, through the thickness of the graphite sheet, and through the layer of activated carbon. A detailed description of this optimization procedure will be presented with an example later in this chapter. In the case of the constructed apparatus described in Fig. 2.5, we have established a good compromise for the present density of graphite sheet (1,390 kg·m^{-3}): the thickness of 0.6 mm, separated by a 2 mm space filled with adsorbent particles. This corresponds to a volume fraction of graphite sheets of about 20 %, much lower than all the values considered so far for the dispersion of conductive particles in the absorbent.

The effective conductivity of this composite material is about 600 times greater than that of a classical adsorbent bed. Meanwhile the global permeability of the composite module is hardly influenced, since the gas passes mainly through the activated carbon particle layers.

Then one may ask: *Is this the best configuration? Can the heat transfer be further enhanced by geometric optimization?*

On one hand, the graphite sheets could be further compressed, leading to even higher compactness with equal heat flux transported. On the other hand, the heat transfer in the perpendicular direction with respect to the graphite layers is still limited, because of the bad adsorbent/graphite contact and the very low conductivity of the particle bed. This situation could be improved for example, by adding "fins" perpendicular to the graphite layers while still keeping the 20 % volume fraction, as shown in Fig. 2.3.

One important limitation of this approach concerns the fabrication technique. Evidently, a certain degree of thermal performance loss would be acceptable if a fast and effective mode of fabrication was available. For the implementation of highly compacted graphite sheets, this remains to be investigated. For metals, we can consider all existing structures, such as foams, sponges or folded metals. The most promising way seems to be the extrusion of a metal having thermal properties close to the graphite.

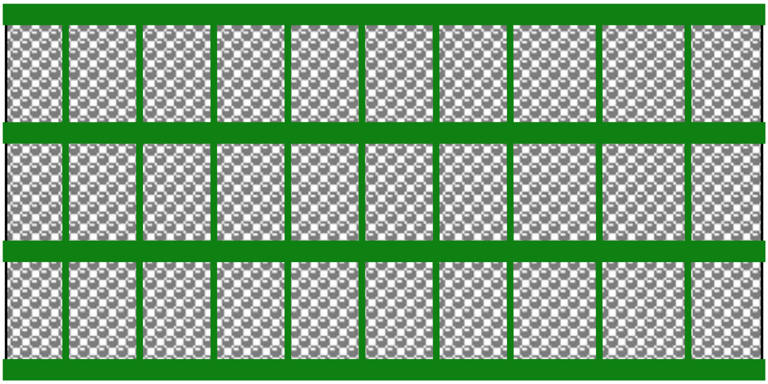

Fig. 2.3 The configuration of the active composite with fins (Luo 2001)

2.2.2 *Use of Thermoelectric Elements*

Having proposed the shape of adsorbent bed with enhanced heat transfer characteristics, another issue that should be considered for shortening the cycle duration is the mode of energy supply/evacuation, since it is known that adsorption is exothermic so that it releases heat while desorption is endothermic which absorbs heat. Conventionally, the working gas will be pre-heated or cooled before entering the absorbent bed. Other methods include the integration of tubular heat exchangers or the use of Joule effect (Electro-thermal swing adsorption that will be presented after).

I first proposed the idea of using thermoelectric elements (TE) to produce the temperature variations of the adsorbent bed. Firstly, let us give a brief introduction on the basic principle of TE.

A TE is a device that provides the direct conversion of temperature differences to electric current or vice versa: it creates an electric current when there is a temperature difference between two sides (Seebeck effect), or conversely, it creates a temperature difference when it is fed by an electrical current (Peltier effect). One noticeable feature of the TE is that the thermal polarity of TE depends on the polarity of applied current: the cold junction and the hot junction can be changed easily by reversing a DC current. As a result, the TEs are efficient temperature controllers.

The TE I used in my research is a conventional type with the dimension of 62 × 62 mm. It consumes 3–14 A at 12 V, the electric power then being about 100 W. The temperature difference between two faces depends on the pumped power, with the maximum temperature at hot face at about 70 °C. Note that TEs with higher maximal temperature are now commercialised. The thermal power of the TE is in the order of 100–200 W depending on the temperature difference, corresponding to the power pumped by the adsorbent composite.

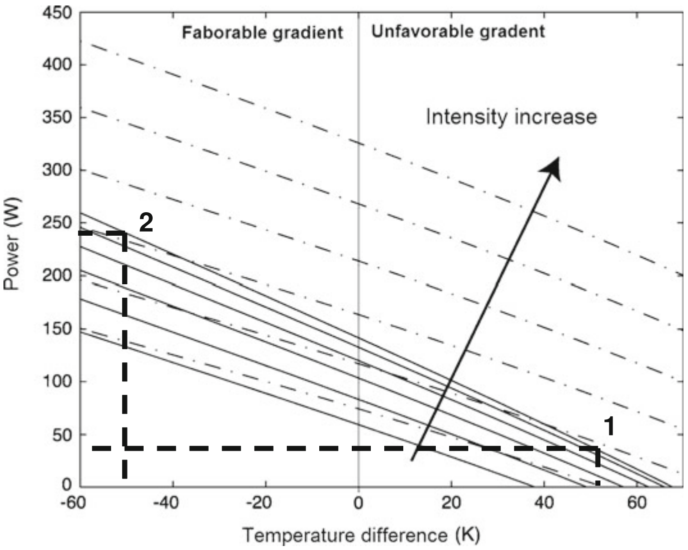

Fig. 2.4 Cooling power (*solid line*) and heating power (*dotted line*) as a function of temperature difference between two faces for different values of electric current (4–14 A) (Luo 2001)

I emphasize the originality of using TE in the context, related to the periodic operation. In fact, I am going to alternatively heat and cool the adsorbent bed by contacting it with one face of TE. To periodically inverse the thermal polarity, it is just necessary to inverse periodically the electric polarity. Thanks to the fast dynamics and easy controllability of TE, the temperature switch occurs in a matter of *seconds* after inversion of the electric current.

The advantages are not limited to this. Figure 2.4 shows the heating and cooling power as a function of the temperature difference between the two faces. For a normal operation of the element (no electric polarity inversion, steady state, ΔT positive), the thermal power is maximal when the ΔT is zero, and the thermal power decreases to zero when ΔT increases to the maximum value. When working under periodical regime, since ΔT will be negative when inversing the element's electric polarity, it will be operated with a negative thermal gradient. For example, under the steady state with a ΔT of 50 °C, we will have a maximal cooling power of about 50 W (point 1 in Fig. 2.4). By inversing the polarity, the initial ΔT is thus -50 °C, corresponding to a power of about 240 W (point 2 in Fig. 2.4). Of course, the temperatures will then evolve to the imposed values, and the ΔT and cold power will reach their values under steady state, till the next inversion of polarity.

Operating in transient state by successively inversing the polarity permits an intensification of the cooling power of the thermoelectric elements.

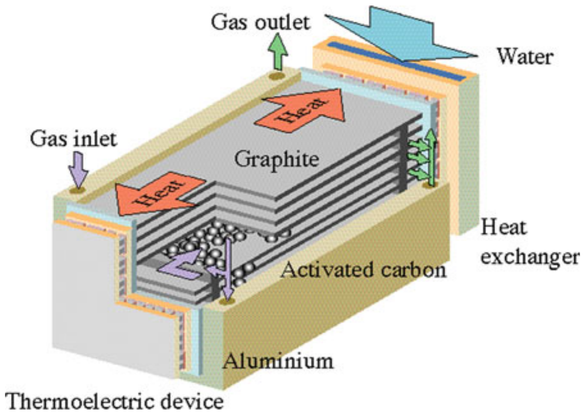

Fig. 2.5 Overall view of adsorption column with thermoelectric devices. Outer polypropylene wall not shown (Bonnissel et al. 2001b). Published with kind permission of © AMERICAN CHEMICAL SOCIETY 2001. All rights reserved

Note that there are a number of distinctive features of TE, as I discussed above, but the energy "dissymmetry" character should not be ignored. This results from the dissipative effects (Joule effect) so that the heating power is always much higher than the cooling power (Fig. 2.4). For the actual operation of TSA apparatus, this dissymmetry has to be accounted for by a pertinent operation mode that will be presented below.

2.2.3 Periodic Operation Modes

Figure 2.5 presents the configuration of the adsorption apparatus we designed, optimized, fabricated and tested, in view of small scale applications (Bonnissel et al. 2001b). It is composed of a parallelepiped of polypropylene with two aluminum plates on two opposite faces. Two TEs are pressed onto these plates by two brass heat exchangers. The adsorption bed consists of parallel and regularly spaced thin graphite sheets with high thermal conductivity separated by spacing slabs (permeable to gas flow) and enclosing activated carbon pellets.

The energetic analysis of the system is complicated because of the variability and the coupling of all system parameters, and also of the asymmetry of the heating and cooling. Because of the Joule effect, it is also possible to use a lower intensity in heating period of the adsorbent than in the cooling period. Furthermore, the durations of the cooling and heating cycles are not necessarily equal.

I present an example of separation process realized with such a system. The column is fed by a mixture of helium-CO_2 (17 %) at a constant flow rate of 30 $mL\cdot s^{-1}$. No purge step with pure inert gas is used. The TEs are electrically cycled as explained above. Cooling produces adsorption while heating produces desorption. Figure 2.6 shows the time variations of the measured and calculated temperatures in the adsorption column. The experiments consisted of adsorption periods of 10 min at a temperature set point of −10 °C and desorption periods of

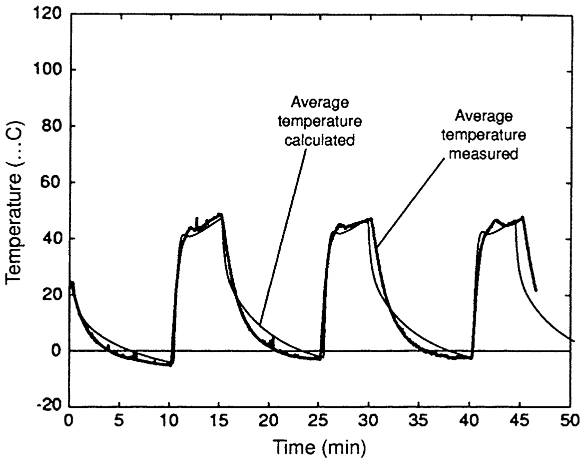

Fig. 2.6 Experimental and calculated temperature variations with time; water temperature, 25 °C; adsorption, 10 min at −10 °C; desorption, 5 min at 60 °C (Bonnissel et al. 2001b). Published with kind permission of © AMERICAN CHEMICAL SOCIETY 2001. All rights reserved

5 min at a temperature set point of 60 °C. The mean temperature of the active composite varies between −5 and 50 °C.

Figure 2.7 shows the measured and calculated outlet carbon dioxide concentrations with time for an experiment with a 17 % CO_2 molar inlet concentration. During the cooling (adsorption) period, the CO_2 concentration decreases rapidly and later slowly increases because of breakthrough of the adsorption front. During the heating (desorption) period, the CO_2 concentration increases very quickly and then decreases, when the bulk of the CO_2 has been desorbed.

Note that the duration of the entire cycle is about 25 min, which is actually a very rapid TSA process with respect to classical TSA cycles in hours.

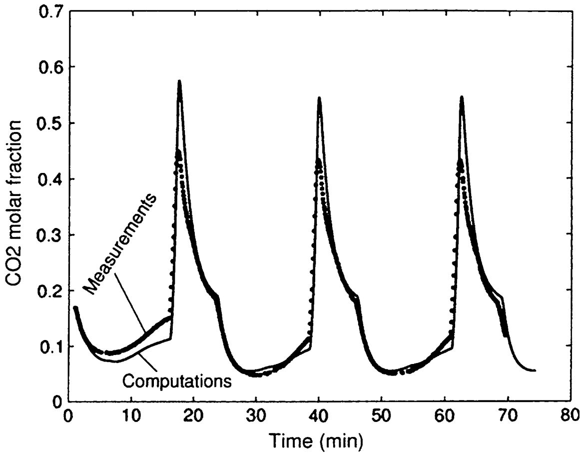

Fig. 2.7 Mole fractions of CO_2 of the adsorption–desorption cycles (Bonnissel et al. 2001b). Published with kind permission of © AMERICAN CHEMICAL SOCIETY 2001. All rights reserved

2.2.4 Cycling-Zone Adsorption

For the adsorption/desorption cycle tested here, the mixture of CO_2 and He is fed continuously to the adsorbent bed, neither with flow reversal nor use of purge gas. In fact, this operating mode is inspired by the work of Jacob and Tondeur (1983a, b) which showed that, under certain conditions, a pure helium flow could be obtained. However, the present experimental results (Fig. 2.7) merely show that a concentration/depletion process is possible with short cycles in one shallow column. This limitation may be due to the small bed length and probably to a poor chromatography quality. Nevertheless, the flow-rate used here is on the order of 0.1–0.14 $m^3 \cdot h^{-1}$. A larger flow-rate increases the spread of the residence time distribution and thus diminishes the chromatographic quality.

Could the operation mode be further optimized in order to approach a total separation?

Firstly, I considered using a parallel-series arrangement of similar modules, as illustrated in Fig. 2.8. The parallel setup allows for a larger flow to be processed at a similar gas velocity, and the series setup allows for an improvement in separation quality.

Then, *cycling-zone adsorption* was used. This operation mode was introduced by Pigford in the late 1960s (Pigford et al. 1969; Baker and Pigford 1971). It involves periodic change of temperature of a series of columns, with a phase shift between successive columns. Figure 2.9a gives schematically the temperature distribution of a series of five columns at three different phases in such a process.

I simulated the operation of such a series of five columns, under conditions comparable to those of Fig. 2.7 (20 % CO_2; flow-rate 30 $mL \cdot s^{-1}$; heating 30 min at 60 °C; cooling 10 min at −10 °C). The result is shown in Fig. 2.9b. It is clearly seen that the separation is amplified in each column, and an effluent having a very low fraction of CO_2 is obtained already in column 3. The effluent of the fifth

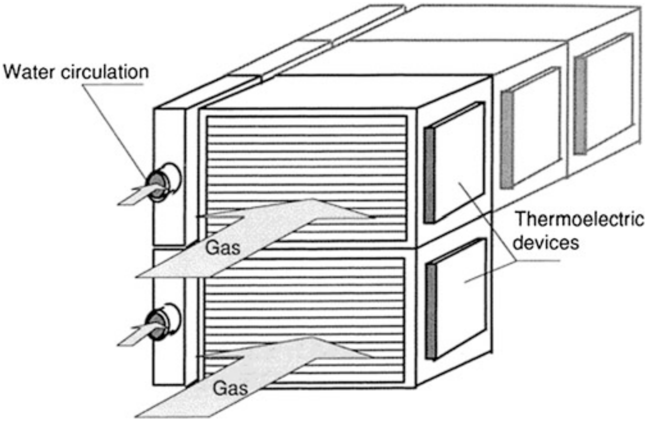

Fig. 2.8 Series–parallel arrangement of adsorption modules (Bonnissel et al. 2001b). Published with kind permission of © American Chemical Society 2001. All rights reserved

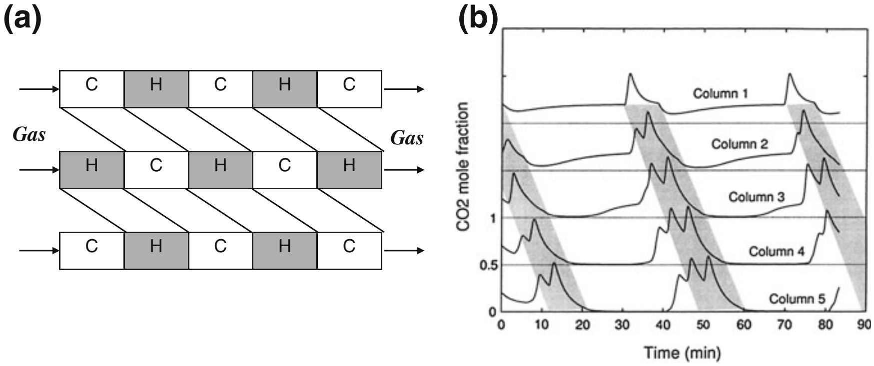

Fig. 2.9 Cycling-zone adsorption. **a** principle of temperature shifts in five-column cycling-zone adsorption; **b** simulation of outlet concentrations (Bonnissel et al. 2001b). Published with kind permission of © American Chemical Society 2001. All rights reserved

column contains less than 0.1 % CO_2 for 20 min, while in the effluent of the other 20 min CO_2 concentration is doubled (average 40 %).

Notice that this operating mode (the so-called direct mode of cycling-zone-adsorption, whereby the columns are heated and cooled through the walls) is hardly possible by other means than those used here, which allows for a relatively fast temperature change in each column and the separate control of each column. It is certainly an operating mode adapted to this technology.

2.2.5 *Short Summary*

I have shown in this section the possibility of a rapid TSA process. It is based on a composite adsorbent bed, composed with layers of activated carbon particles separated by sheets of a highly conductive graphite material. The geometry of the graphite material may have a multi-scale structure and optimized based on its heat and mass transfer characteristics. It also uses thermoelectric elements to alternatively heat and cool the adsorbent bed. The high effective conductivity of the bed and the fast dynamics of the thermoelectric elements allows cycles (cooling and adsorption/heating and desorption) to be run in 10–20 min. The series–parallel arrangement of adsorption column and the cycling zone operation mode can further amplify the separation in terms of both throughput and separation quality.

2.3 Other Intensified Adsorption Processes

To periodically modulate the temperature of the adsorption column is not the only method to intensify the adsorption process. In this section, I will present and discuss other adsorption processes that I have developed or investigated, to intensify the separation subject to different contexts. These adsorption processes are:

- Pressure Swing Adsorption (PSA);
- Electrothermal Swing Adsorption (ESA);
- Adsorption in Circulating Fluidized Bed (CFB)

2.3.1 Pressure Swing Adsorption

As the name suggests, the external parameter modulated here is the pressure, a parameter that can be varied rapidly. One typical application is the purification and production of hydrogen from natural gas reforming followed by water–gas shift reaction. Hydrogen can be produced by PSA with a high purity (99.999 %) by adsorption of impurities on a layer of activated carbon (CO_2, CH_4, other heavy impurities) followed by a layer of zeolite (CO, N_2, essentially) (Chlendi and Tondeur 1995).

Figure 2.10 presents the principle of a simple PSA cycle, whose four stages in the cycle take place on the same adsorption column, and which therefore necessities an auxiliary reservoir where intermediate products may be stored between stages. These four stages are: (1) pressurization of the column from low pressure to high pressure; (2) isobaric production; (3) depressurization; (4) isobaric purge by using a fraction of the product of the second stage, and during which impurities are desorbed at low pressure. No auxiliary gas is therefore necessary in this process whose driving energy is the compression of the gas mixture to be separated. Note that the purge duration is not necessarily equal to the adsorption duration. Our study (Bonnot et al. 2006) showed that an optimal purge duration may exist, of the order of 80 % of the adsorption duration.

It is interesting to compare the TSA with the PSA from the point of view of intensification. The key feature of PSA is that it is *extremely productive* for the separation of *light gases*. The characteristic cycle duration of a PSA is about several minutes, or even several seconds for rapid PSA processes, with respect to several hours for classic TSA processes. In fact, the PSA is a process intrinsically intense. The reason lies in the fact that it is relatively easy to quickly increase, respectively decrease, the pressure in an adsorption column by pumping compressed gas into it, respectively releasing gas from it.

Unfortunately, the rapid PSA is not always possible. When heavier molecules are adsorbed on charcoal or zeolite, the desorption stage will be inefficient without raising the temperature, or without vacuum (which then makes the cycle duration considerably longer). In addition, a simple PSA such as that described in Fig. 2.10 may imply a significant loss of useful product, which is discarded with the blowdown and the purge. When a high recovery is sought, as in the case of hydrogen, multiple columns (up to 12 or 16 columns for example) and complex cycles are needed, and the PSA is then much less compact. None of the TSA process has such complexity. In general, it has a maximum of 2 or 3 columns.

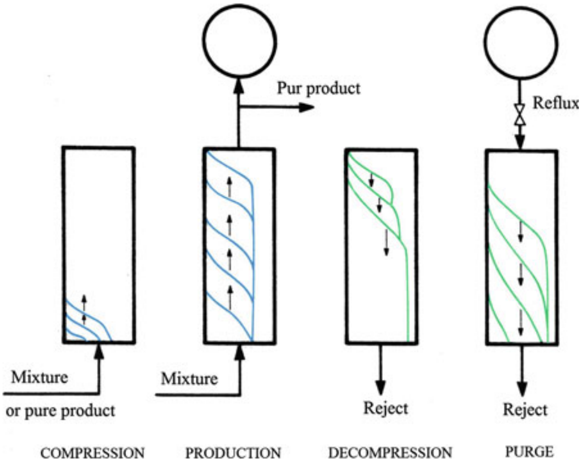

Fig. 2.10 Principle of a PSA cycle (Luo 2001)

The different features of the two processes determine their different position and application domains in industry. The PSA is often an autonomous separation operation which provides final products (dry air, nitrogen, pure oxygen, etc.). The TSA on the contrary is rather a non-autonomous purification operation; the impurities separated from the main stream must be further treated (condensation, distillation or incineration for the solvents for example).

Then one may ask: *Can PSA and the TSA complement each other?*

In fact they cannot in general. The application domains and conditions are different. But the question may be formulated in another way: *Since the PSA has a high productivity, can we in certain cases, replace a TSA process by a PSA?*

The key issue is the possibility of efficient desorption by pressure decrease. With strongly adsorbed species at ambient temperature, this is impossible. In fact, we may then imagine the replacement of a TSA by a PSA functioning at a mean temperature higher than the ambience. Then the problem is to determine an optimal mean temperature, which is a compromise between good adsorption (favored by lower temperature) and a good desorption (favored by higher temperature). Such a process seems interesting if the gas to be treated is available at a temperature higher than ambience, the case of reforming gas for example. Some efforts have been devoted to this technique recently (e.g. Gales et al. 2003; Sharma and Wankat 2009).

This coupling can be considered as intensification with respect to PSA (its temperature optimization), as well as with respect to TSA (to be replaced by a PSA at none-ambient temperature).

2.3.2 Electro-Thermal Swing Adsorption

For VOCs recovery, TSA has some limitations: desorption by hot gas leads to low concentrations of desorbed vapours which make the condensation difficult; desorption by steam is usually reserved to VOCs which are not miscible with water in order to avoid subsequent distillation of the mixture. Even when the VOCs are to be destroyed by incineration, rather then recovered, they should be produced at a concentration high enough to allow autothermal incineration (without addition of fuel).

In order to avoid these inconveniences, the so-called *Electrical Swing Adsorption* (*ESA*) could be an alternative. Direct-electrothermal regeneration by the direct Joule effect uses the adsorbent as an electrical resistor to heat and regenerate the adsorbent. This idea is not new, and was first proposed by Fabuss and Dubois (1970). Since then, many studies have considered different aspects of the concept (e.g. Petkovska et al. 1991; Saysset et al. 1999; Subrenat et al. 2001; Cheng et al. 2002; Sullivan et al. 2004; Yu et al. 2004, 2007; Luo et al. 2006, etc.).

Besides the adsorption and regeneration, vapour condensation is necessary to recycle liquid solvent or for its possible transport to a reprocessing plant. We propose the use of TE, as we have introduced for intensified TSA process, which functions as a rapid cooler or as a heater (by simply reversing the current direction). These elements have very small thermal inertia and permit obtaining negative temperatures very rapidly (in several seconds). In case of crystallization, these devices can also be unclogged easily by melting with the inverse of the current within a few minutes.

The principle of the compact and integrated process is illustrated in Fig. 2.11. It consists of an adsorption column for the concentration of VOCs and a TE condenser for the liquefaction of the desorbed vapour during the regeneration. The

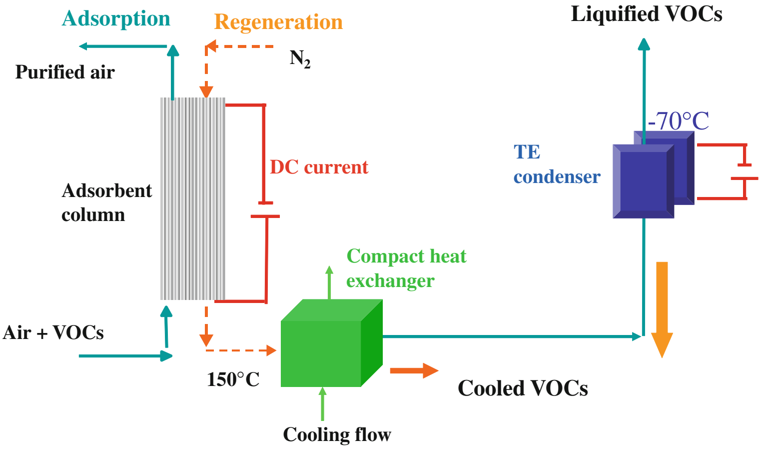

Fig. 2.11 Principle of the integrated ESA process for VOC concentration and recycling

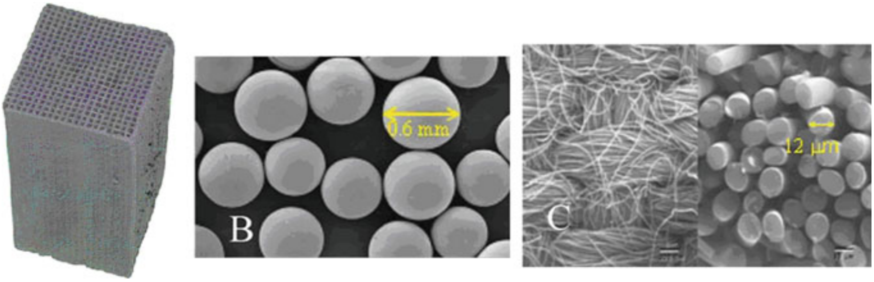

Fig. 2.12 Photos of ACM, ACB and ACFC (Luo et al. 2006). Published with kind permission of © ELSEVIER 2006. All rights reserved

installed compact heat exchanger serves as pre-cooler or part of condenser, depending on the temperature of the working fluid.

Once this process is envisaged, the next step is the search for a suitable adsorbent for ESA usage. Although granular activated carbon is the most common morphology used to adsorb VOCs from gas streams, commercial activated carbons are now available in a variety of forms, such as monoliths (ACM), spherical beads (ACB) and fiber cloths (ACFC), as shown in Fig. 2.12. ACM is generally made of powdered activated carbon mixed with water and an organic binder. The mixture is then extruded at high pressure and dried between 400 and 500 °C to form a monolith. ACB is a synthetic carbonaceous adsorbent produced by pyrolysis of a highly sulfonated styrene divinylbenzene resin, and activated between 300 and 1,200 °C. Pyrolysis and activation increase the microporosity of the beads, while only providing a small increase in the samples mesoporosity. ACFC are woven

Table 2.3 Physical, electrical, adsorption and cost properties of ACM, ACB, and ACFC (Luo et al. 2006)

Adsorbent Model	ACM RICD, Beijing, China	ACB Ambersorb 572 (Rohm and Hass)	ACFC ACFC-5092-20 (American Kynol Inc.)
Pressure drop at 0.1 m/s of superficial gas velocity (Pa/cm)	1.0	89.9	38.8
Permeability (m^2)	1.8×10^{-8}	2.0×10^{-10}	1.9×10^{-11}
Micropore volume (cm^3/g)	0.21	0.41	0.75
Adsorption capacity at $p/p_o = 0.9$ (g/g)	0.26	0.52	0.6
Throughput ratio	0.81	0.91	0.81
Length of unused bed	0.21	0.08	0.21
Electrical resistivity at 455 K (Ω-m)	3.9×10^{-1}	8.1×10^{-2}	4.8×10^{-3}
Max. achieved concentration factor	46	20	1,050
Cost ($/kg)	3.6	1,575	730

Published with kind permission of ELSEVIER © 2001. All rights reserved activated carbon fibers made by pyrolysis of cellulose, rayon, polyacrylonitrile or saran fibers, etc.

A comparative study is carried out to better compare their physical, electrical and adsorption properties. Batch operation experimental results are listed in Table 2.3. We briefly conclude that the ACM has the lowest pressure drop, highest permeability, highest electrical resistivity and lowest cost; the ACB has the largest throughput ratio and lowest length of unused bed, whereas the ACFC shows the largest adsorption capacity for toluene, fastest to regenerate and largest concentration factor. A detailed comparison may be found in Luo et al. (2006).

With a compromise between adsorption/regeneration performance and cost, we employed an ACM in the experimental test of ESA of toluene. The shape is a parallelepiped of 10 cm in length and a square cross-section of 5 cm by 5 cm. It contains 400 longitudinal parallel channels of square cross-section of 2 mm by 2 mm. The wall thickness between the channels is 0.5 mm, as shown in Fig. 2.12. The BET surface area is about 615 $m^2 \cdot g^{-1}$. A high adsorption capacity (up to 2.5 $mol \cdot kg^{-1}$) at low partial pressures of toluene at room temperature is observed, implying that it is effective for cleaning the gas.

2.3.3 Adsorption in Circulating Fluidized Bed

Circulating fluidized bed (CFB) technology is a process for clean combustion and incineration because of its good heat and mass transfer capabilities. *Could this technology be extended to the adsorption processes?*

If this was possible, the advantages are numerous. Besides the intensified heat and mass transfer between fluid and solid particles, it allows a continuous (or pseudo-continuous) operation, thus avoiding the immobilization of saturated adsorbent, which typically occurs in fixed bed operations. In addition, the fluidized bed operation allows high fluid flow-rate with relatively small pressure drops and reduced blockage risk for the treatment of dusty gases or slurries.

Despite these advantages, CFB techniques, although classic in catalysis, are hardly used in adsorption, mainly for two reasons:

- Attrition: turbulent transport of classic adsorbents (e.g., activated carbon) subjects the particles to strong attrition forces, resulting in adsorbent degradation and dusting; attrition resistance then becomes an important requirement;
- Purity requirement: many adsorption processes require high purities, implying a large number of "theoretical stages", which can only be offered by fixed bed.

Under certain circumstances, these factors are not prohibitive, and I have therefore explored the potential application of CFB technique in adsorption. The first requirement is an adsorbent resistant to attrition. Ambersorb 600 made of carbonized polymer material obtained from Rohm and Haas, Philadelphia, PA, USA, satisfies this condition. It is in the form of small spherical beads with

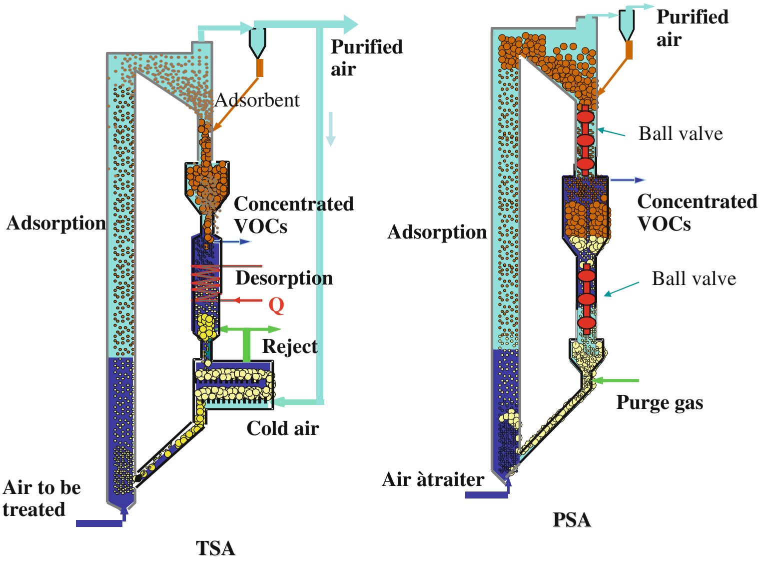

Fig. 2.13 Schematic of continuous TSA or PSA processes using circulating fluidized bed technique

uniform particle diameter and high crush strength (>1 kg/bead), desirable for fluidized bed application.

Figure 2.13 shows the design of TSA and PSA processes for the treatment of VOCs using CFB technology. In the TSA process, the desorption section is heated by a heat exchanger. In the PSA process on the other hand, the pressure change between the adsorption section and the desorption section is managed by a system of ball valves.

Batch type experiments were run (Song et al. 2005) in which the solid is fluidized but does not circulate. The results are thus comparable to that of a fixed bed, with a breakthrough curve. Such curves were found to be relatively sharp, allowing for efficient VOCs abatement: the reduction of toluene from 460 to 5 ppm on less than one meter of bed height. The predicted performance in a continuous mode where the adsorbent would be partially regenerated implies a less-than-total toluene abatement.

2.4 Design of Structured Porous Medium for Gas Adsorption or Storage

I have underlined in earlier sections the importance of the shape or morphologies of porous media for the adsorption or gas storage processes. In fact, the optimal design of such porous material must account for the following factors:

- High static gas adsorption/storage capacity per unit volume, implying a large volume of nano-porous space where adsorption, condensation, or chemical reaction takes place.
- Fast transfer kinetics from the nano-pores to the storage outlet; reciprocally, the filling of the storage/adsorption tank should be possible in a short time. Unfortunately, the pure diffusional mass transfer in the nano-porous is extremely slow. The properties expected therefore imply that some intermediate porous network be distributed in the porous media, to allow rapid transport of the gas molecules to the nano-pores. This intermediate porous network should occupy a small volume, because it contributes little to the storage capacity, and should also generate low pressure drop.
- Adsorption being strongly exothermic, the heat released during the filling of the storage should be rapidly and efficiently removed, to avoid the decrease of the storage capacity, and vice versa for the desorption cycle. Thus, the packing should constitute a continuous heat conducting material, and/or incorporate some "conduction promoters", so that the heat may be removed through the walls of the vessel for example.

In earlier sections, I have presented the efforts on the property modifications of porous media to enhance the heat and mass transfer, including the insertion of conductivity promoters and the employment of new adsorbent morphologies (ACM, ACB, ACFC, etc.). Of course, the available shapes and inner structures of the porous media are limited because of the fabrication constraints. Then one may ask: *Is it possible to theoretically design a multi-scale structured porous material and a system having properties I have evoked above for efficient gas adsorption and storage?*

To answer this question, I will present here a theoretical optimization approach based on the equipartition property (here the characteristic transport time). At this stage, a full theoretical development is not available, but I shall illustrate the principles on which it could be based.

2.4.1 Definition of Elemental Domain

As a starting point, let us first define an elementary domain, which may very well be the smallest scale accessible by fabrication, and/or the scale at which the elementary phenomena occur, here say adsorption and nano-porous mass transport.

Consider the cylindrical volume of Fig. 2.14, composed of homogeneous nano-porous material, in which gas is transported by a mechanism of surface diffusion described by a constant diffusivity α_0. The cylinder (length L_1 and radius r_1) is "irrigated" by a central micro-pore, in which diffusion occurs with a diffusivity $\alpha_1 > \alpha_0$. It is assumed that all the gas moleculars contained in the cylinder must enter or exit through one end of this micro-pore (the other boundaries are closed). In addition, it is assumed that diffusion in the nano-porous region may be

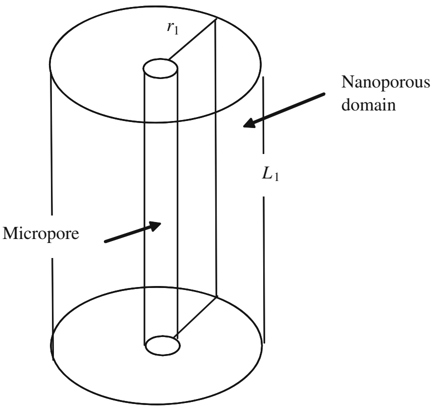

Fig. 2.14 Cylindrical elementary domain (Luo and Tondeur 2005). Published with kind permission of © ELSEVIER 2005. All rights reserved

considered as one-dimensional as if all nano-pores were oriented radially. The latter assumption is a good approximation when α_1 is much larger than α_0, or when the nano-pore network is actually anisotropic.

I use here an approach based on characteristic times, defined as the ratio of the square of a characteristic dimension to the diffusivity. The characteristic times are analogous to resistances and the inverse of conductances, in the sense that they are additive for mechanisms that are in series. For example, for the nano-porous space the local characteristic time of radial diffusion to the micro-pore at a distance x from the micro-pore is x^2/α_0. The average $\bar{t}_0$ of this quantity taken over the nano-porous domain is simply obtained by integrating over x from 0 to r_1 (the thickness of the micro-pore is neglected for simplicity, and the other space variables are not necessary owing to the symmetry of the domain and the assumption of pure radial diffusion).

$$\bar{t}_0 = \frac{1}{r_1}\frac{1}{\alpha_0}\int_0^{r_1} x^2 dx = \frac{r_1^2}{3\alpha_0} \tag{2.1}$$

Similarly, the diffusion time in the micro-pore, considered mono-dimensional in the direction y is given by:

$$\bar{t}_1 = \frac{1}{L_1}\frac{1}{\alpha_1}\int_0^{L_1} y^2 dy = \frac{L_1^2}{3\alpha_1} \tag{2.2}$$

The mechanism assumed here is purely sequential: for desorption, the molecules must first diffuse in the nano-space, then in the micro-pore (or conversely for adsorption). The average total time τ_1 is the sum of the two "partial" times:

$$\tau_1 = \bar{t}_0 + \bar{t}_1 \tag{2.3}$$

For a specified volume of the domain, i.e. a specified value of the product $V_1 = \pi L_1 r_1^2$, one can calculate a value of the "aspect ratio" L/r that minimizes the average total time. This is done for example by eliminating r_1 using the constraint V_1, then differentiating τ_1 with respect to L_1 (also verifying that the second derivative is positive). One then finds:

$$\left(\frac{\partial \tau_1}{\partial L_1}\right)_{V_1} = -\frac{V_1}{3\alpha_0 L_1^2} + \frac{2L_1}{3\alpha_1} = 0 \tag{2.4}$$

A number of remarkable relations result from this optimization, such as:

Optimal aspect ratio:

$$\frac{L_1}{r_1} = \left(\frac{\alpha_1}{2\alpha_0}\right)^{\frac{1}{2}} \tag{2.5}$$

Average transfer times:

$$\frac{\bar{t}_1}{\bar{t}_0} = \frac{1}{2} \text{ and } Min\, \tau_1 = \frac{3}{2}\bar{t}_0 \tag{2.6}$$

2.4.2 Multi-Scale Construction

Suppose now that I assemble a number of n_1 elementary domains such as the one I just investigated together in such a way that the "mouth" of every micro-pore opens on a "meso-pore", where the transport is still diffusional, but with a still larger diffusivity α_2 and an average transport time of $\bar{t}_2$. This construction process is illustrated in Fig. 2.15. Clearly, for this construction to make sense and for the resulting structure to be compact, the elementary domains should have a non circular shape, for instance squares, lozenges or hexagons would be suitable for compact packing. Anisotropic transport may even be accounted for, and an optimal aspect ratio of the cross-section may be defined. The simplicity of the above equations is then lost, but it is still possible to develop a similar calculation and define average transport times for this new elementary domain.

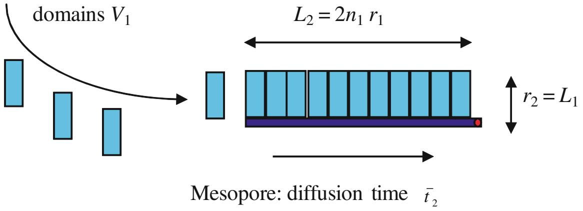

Fig. 2.15 Constructing the first assembly by elementary domains (Luo and Tondeur 2005). Published with kind permission of © ELSEVIER 2005. All rights reserved

Returning to Fig. 2.15, the width r_2 of this new domain is the length L_1 of the elementary domain, and its length L_2 is n_1 times the width $2r_1$. From the point of view of the meso-pore, the full set of elementary domains behaves as a homogeneous domain with an average transfer time τ_1. A new total transfer time is defined as:

$$\tau_2 = \tau_1 + \bar{t}_2 \tag{2.7}$$

Following the same approach, this quantity may be minimized with respect to the length L_2, in other words, with respect to the number of elementary domains. Considering first n_1 as a rational number (not necessarily integer), relations formally identical to 2.5 and 2.6 are found, where the indices are merely incremented by one. Of course, the nearest integer value of n_1 must be chosen, leading to a slightly sub-optimal construction.

Figure 2.16 illustrates how this "constructal" approach may in principle be extended to still an additional scale. If the transport mechanism in the "macro-pore" is still diffusional, similar recurrent relations may be obtained. An interesting aspect comes up when the transport mechanism changes. For example, let us assume that at the macro-pore level of Fig. 2.16, diffusion no longer governs the transport, but instead advection takes place, with a velocity noted u_3. The total time then becomes:

$$\bar{\tau}_3 = \tau_2 + \bar{t}_3 = \frac{L_2^2}{3\alpha_2} + \frac{L_3}{2u_3} \tag{2.8}$$

The minimization with constraint $V_3 = L_3 L_2^2$ equal to constant leads to a different expression of the aspect ratio:

$$\frac{L_3}{L_2^2} = \frac{2u_3}{3\alpha_2} \tag{2.9}$$

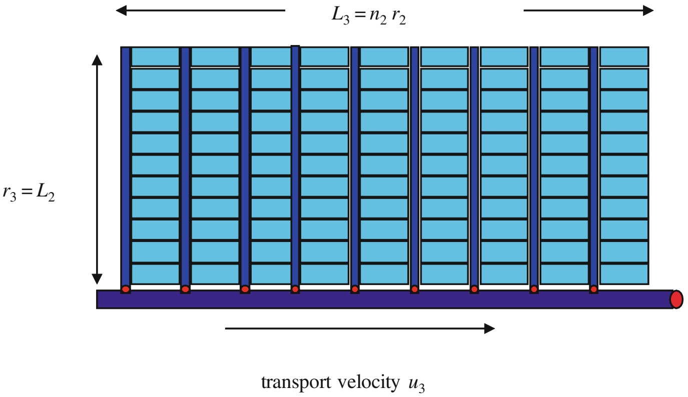

Fig. 2.16 Constructing the second assembly by several first assemblies (Luo and Tondeur 2005). Published with kind permission of © ELSEVIER 2005. All rights reserved

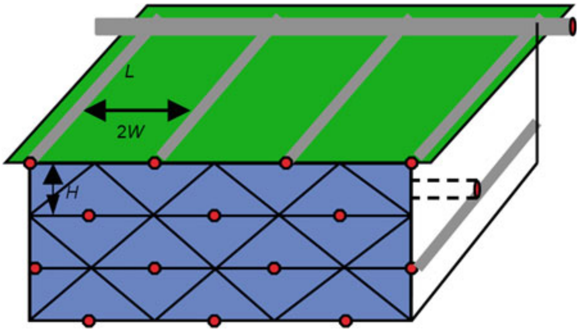

Fig. 2.17 Arrangement of heat conducting tubes and sheets in an isolating block (Luo and Tondeur 2005). Published with kind permission of ELSEVIER 2005. All rights reserved

Addressing now briefly the 3D packing problem, it is clear that one cannot be satisfied with the considerations above, and one of the research challenges is to design real 3D systems. Figure 2.17 illustrates the sort of design one is led to. This figure illustrates how heat pipes or heat conducting rods may be combined with heat conducting sheets to “move” the heat into or out of a three-dimensional poorly conducting structure. The diamond-pattern appearing on the front face may be optimized to account for anisotropic conduction in the W and H directions.

This way of building a multi-scale structure by successive optimization from the smallest scales to the largest is typical of the “constructal approach”, developed by Bejan and co-workers (1997, 1998, 2004 for example). It is based on the assumption that this sequential optimization furnishes the overall optimal, which turns out to be a very reasonable assumption when the processes involved are in series.

2.5 Concluding Remarks

In this chapter, I have presented and discussed various adsorption processes subject to specific application domains and conditions. The thermodynamic parameter modulated could be the temperature (TSA), operating pressure (PSA) or electrical current intensity (ESA). Various technical or operational methods have been introduced, aiming at intensifying the adsorption in porous media. Due to the cyclic nature of these swing processes, the main aspect of intensification is to accelerate the dynamics and to shorten the cycle time by the use of compacted graphite sheet with high thermal conductivity to enhance heat transfer; of thermoelectric elements with less thermal inertia; of careful choice of adsorption/desorption interval; of pressure swing; etc. This we may call “temporal intensification”, but of course, other aspects are also involved, for example:

- *Productivity intensification*: novel morphologies of activated carbon with high adsorption capacity (ACM, ACB, ACFC) or high attrition resistance; circulating

fluidized bed with large gas velocity (throughput); coupled TPSA for purification; series–parallel arrangement; cycling-zone mode; etc.
- *Compactness intensification*: integrated systems; laminated (or more compact) structure of active composite; simplified PSA; etc.

Besides these intensification methods, we also presented in the last part of this chapter, a design and optimization approach for multi-scale structured porous materials and systems for efficient gas adsorption and/or storage. The optimized pore-network provides equitable access of gas molecules to the complete nanoporosity, with minimal space occupied and pressure drop. If it could be realized by modern fabrication techniques, it would have a great potential of application in various processes, with properties of intensified heat and mass transfer.

References

Baker B, Pigford RL (1971) Cycling zone adsorption: quantitative theory and experimental results. Ind Eng Chem Fundam 10:283–292

Bejan A (1997) Constructal theory network of conducting paths for cooling a heat generating volume. Int J Heat Mass Transf 40:799–816

Bejan A, Tondeur D (1998) Equipartition, optimal allocation, and the constructal approach to predicting organization in Nature. Rev Gen Therm 37:165–180

Bejan A, Dincer I, Lorente S, Miguel AF, Reis AH (2004) Porous and complex flow structures in modern technologies. Springer, New York

Bonnissel M, Luo L, Tondeur D (2001a) Compacted exfoliated natural graphite as heat conduction medium. Carbon 39:2151–2161

Bonnissel M, Luo L, Tondeur D (2001b) Rapid thermal swing adsorption. Ind Eng Chem Res 40:2322–2334

Bonnot K, Tondeur D, Luo L (2006) Effects of composition, temperature and purge on the performance of the cyclic adsorption of CO_2 and CH_4 on activated carbon. Chem Eng Res Des 84:192–208

Cheng Z, Yu F, Grevillot G, Luo L, Tondeur D, Yuan WK (2002) Redistribution of adsorbed VOCs in activated carbon under electrothermal desorption. AIChE J 48:1132–1138

Chlendi M, Tondeur D (1995) Dynamic behaviour of layered columns in pressure swing adsorption. Gas Sep Purif 9:231–242

Coste C, Mauran S, Crozat G (1983) Procédé de mise en œuvre de réaction gaz-solide. US Patent 4595774

Douss N, Meunier F (1988) Effect of operating temperature on the coefficient of performance of active-carbon methanol systems. Heat Recovery Sys 8:383–392

Fabuss BM, Dubois WH (1970) Carbon adsorption-electrodesorption process. Proceeding of the 63rd Annual Meeting of the Air Pollution Control Association 70–68:18, St. Louis, Misouri, USA

Gales L, Mendes A, Costa C (2003) Recovery of acetone, ethyl acetate and ethanol by thermal pressure swing adsorption. Chem Eng Sci 58:5279–5289

Grévillot G (1986) Principle of parametric pumping. In: Chereminisoff N (ed) Hand book of heat and mass transfer. Gulf Publication Company, Houston

Guilleminot JJ, Meunier F (1989) Thermodynamic and economic optimization of solar powered solid adsorbent refrigerating units. Int J Solar Energy 7:11–25

Jacob P, Tondeur D (1983a) Non isothermal gas adsorption in fixed beds II non-linear equilibrium theory and guillotine effect. Chem Eng J 26:41–58

Jacob P, Tondeur D (1983b) Non isothermal gas adsorption in fixed beds III Etude expérimentale des effets guillotine et de focalization. Séparation n-pentane iso-pentane sur tamis moléculaire. Chem Eng J 26:143–156

Le Goff P, Tondeur D (1978) La thermo-extraction, un projet d'utilisation des eaux chaudes résiduaires pour séparer les mélanges. Entropie 79:5–17

Luo L (2001) Intensification des transferts en milieux poreux. Mémoire d'Habilitation à Diriger des Recherches INPL Nancy, France. ISBN 2-905267-36-4

Luo L, Ramirez D, Rood MJ, Grevillot G, Hay KJ, Thurston DL (2006) Adsorption and electrothermal desorption of organic vapors using activated carbon adsorbents with novel morphologies. Carbon 44:2715–2723

Luo L, Tondeur D (2005) Multiscale optimization of flow distribution by constructal approach. China Particuology 3:329–336

Petkovska M, Tondeur D, Grevillot G, Granger J, Mitrovic M (1991) Temperature-swing gas separation with electrothermal desorption step. Sep Sci Technol 26:425–444

Pigford RL, Baker B, Blum DE (1969) Cycling zone adsorption, a new separation process. Ind Eng Chem Fundam 8:848–851

Saysset S, Grévillot G, Lamine AS (1999) Adsorption of volatile organic compounds on carbonaceous adsorbent and desorption by direct joule effect. Récents Progrès en Genie des Procédés 68:389–396

Sharma PK, Wankat PC (2009) Hybrid cycles to purify concentrated feeds containing a strongly adsorbed impurity with a nonlinear isotherm: the PSA-TSA supercycle. Ind Eng Chem Res 48:6405–6416

SNEA-LCL (1991) Brevet Europeen WO 91/15292

Song W, Tondeur D, Luo L, Li J (2005) VOC adsorption in circulating gas fluidized bed. Adsorption 11:853–858

Spinner B, Mauran S, Mazet N, Drapier C (1993) Texture, transferts, propriétés mécaniques de blocs poreux anisotropes réactifs vis-à-vis d'un gas. Récents Progrés en Génie des Procédés 7:63–70

Subrenat A, Baléo JN, Le Cloirec P, Blanc PE (2001) Electrical behaviour of activated carbon cloth heated by the joule effect: desorption application. Carbon 39:707–716

Sullivan PD, Rood MJ, Grevillot G, Wander JD, Hay KJ (2004) Activated carbon fiber cloth electrothermal swing adsorption system. Environ Sci Technol 38:4865–4877

Tondeur D, Grévillot G (1986) Parametric ion-exchange processes. In: Ion exchange: science and technology, NATO ASI, 107:369–399

Yu F, Luo L, Grevillot G (2004) Electrothermal regeneration using joule effect on an activated carbon monolith. J Env Eng 130:242–248

Yu F, Luo L, Grévillot G (2007) Electrothermal swing adsorption of toluene on an activated carbon monolith, experiments and parametric theoretical study. Chem Eng Process 46:70–81